





PREX and CREX: Evidence of Strong Isovector Spin-Orbit Interaction

Lie-Wen Chen (陈列文)

School of Physics and Astronomy, Shanghai Jiao Tong University, China

The Symmetry Energy (Esym)
Neutron Skin (Nskin): CREX/PREX Puzzle
Isovector Spin-Orbit Interaction
Summary and Outlook

"International Symposium Commemorating the 40th Anniversary of the Halo Nuclei", Capital Hotel, Beijing, China, October 12-18, 2025



Outline

The Symmetry Energy (Esym)
 Neutron Skin (Nskin): CREX/PREX puzzle
 Isovector Spin-Orbit Interaction
 Summary and outlook



The Symmetry Energy of Nuclear Matter

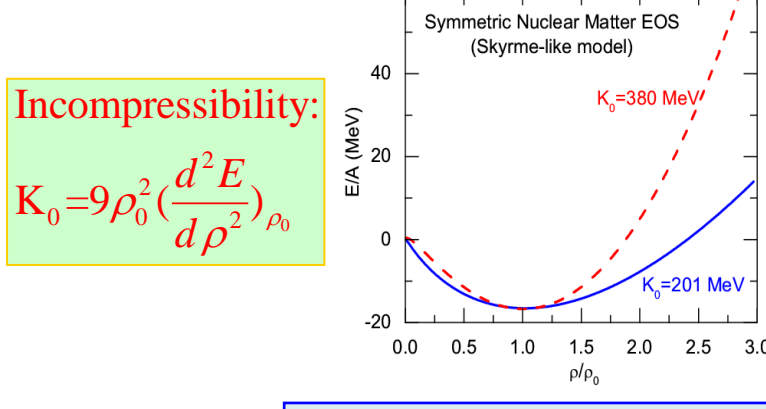
EOS of Isospin Asymmetric Nuclear Matter (Parabolic law)

$$E(\rho, \delta) = E(\rho, 0) + E_{\text{sym}}(\rho)\delta^2 + O(\delta^4), \quad \delta = (\rho_n - \rho_p)/\rho$$

Symmetric Nuclear Matter (relatively well-determined)

→ Isospin asymmetry

Symmetry energy term (largely uncertain)



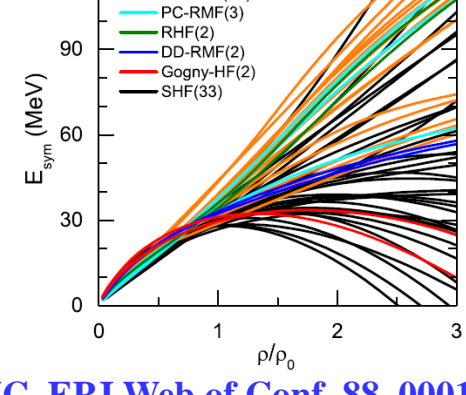
Nuclear Matter Symmetry Energy

$$E_{\text{sym}}(\rho) \equiv \frac{1}{2} \frac{\partial^2 E(\rho, \delta)}{\partial \delta^2}$$

$$E_{\text{sym}}(\rho) = E_{\text{sym}}(\rho_0) + L\chi + \frac{K_{\text{sym}}}{2!}\chi^2 + \frac{J_{\text{sym}}}{3!}\chi^3 + \frac{I_{\text{sym}}}{4!}\chi^4 + O(\chi^5)$$







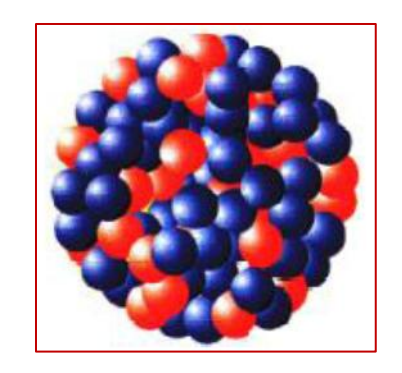
LWC, EPJ Web of Conf. 88, 00017 (2015)

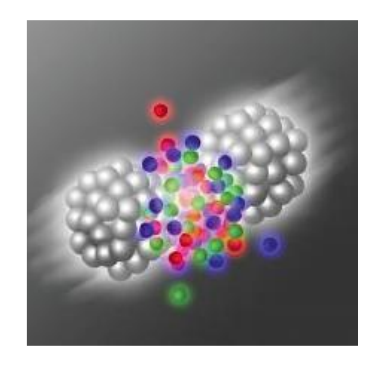
- While the EOS of symmetric nuclear matter is relatively well determined, the density dependence of the symmetry energy is still largely uncertain!
- □ Determining the density dependence of the symmetry energy has been one of the main scientific goals in large-scale scientific facilities of nuclear physics, e.g., CSR/HIAF in China, RIBF/RIKEN in Japan, FRIB/MSU in USA, FAIR/GSI in Germany, RAON in South Korea, ...

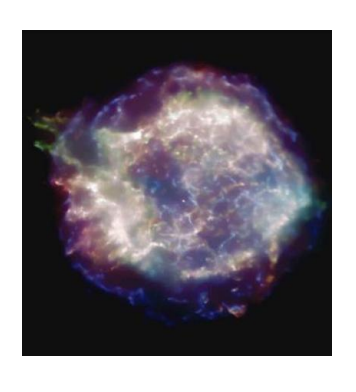


The Symmetry Energy of Nuclear Matter

Isospin asymmetric nuclear matter may exist in various systems in nature











Nuclei

Heavy-Ion Collisions

Supernovae

Neutron stars

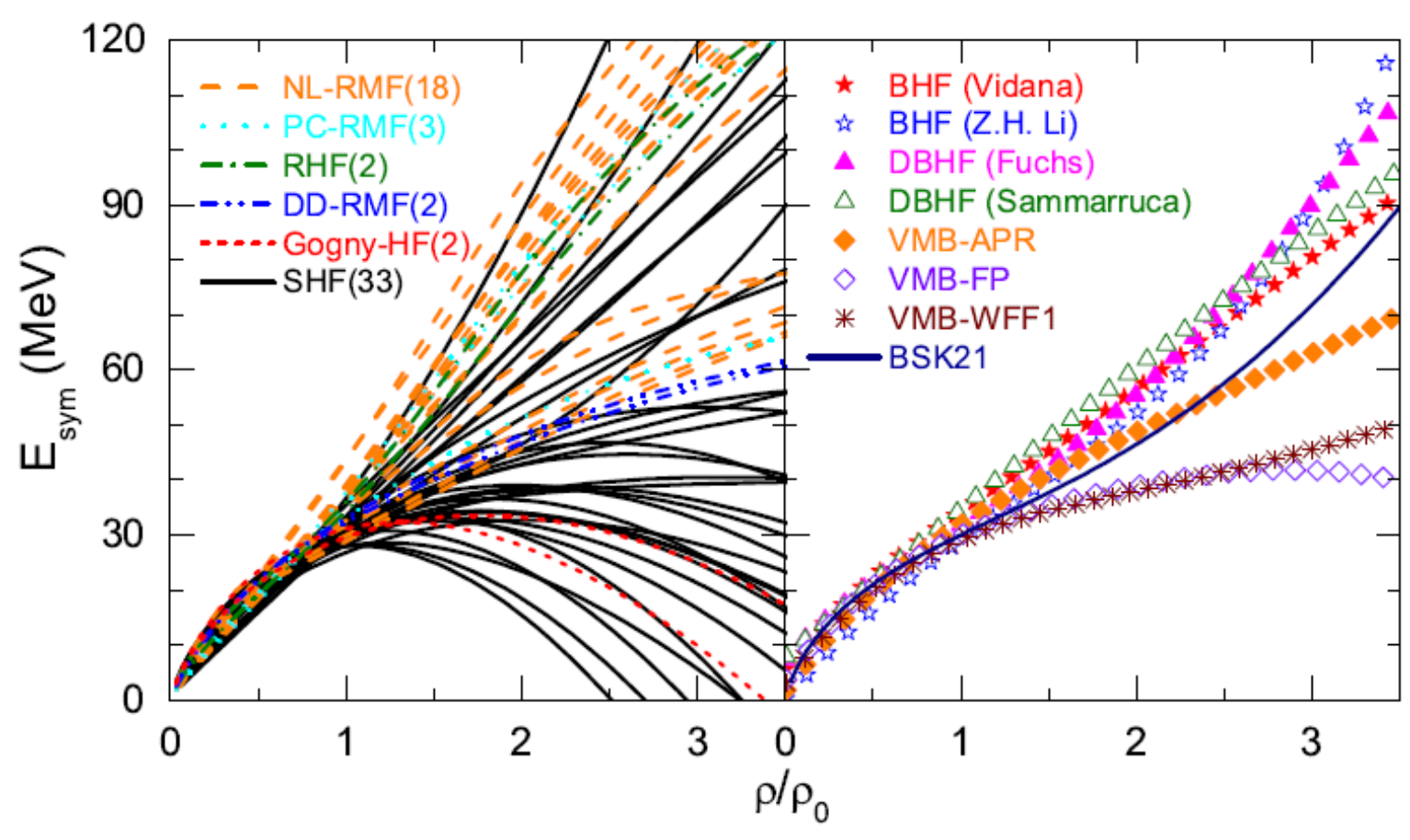
NS Merger

Esym plays a critical role in many issues of nuclear physics and astrophysics!



Esym: Many-Body Approaches





Theoretical predictions of Esym is quite uncertain, especially at high densities!



Esym: Experimental Probes

Promising Probes of the $E_{sym}(\rho)$

(an incomplete list!)

At sub-saturation densities (亚饱和密度行为)

- Sizes of n-skins of unstable nuclei from total reaction cross sections
- Proton-nucleus elastic scattering in inverse kinematics
- Parity violating electron scattering studies of the <u>n-skin</u> in ²⁰⁸Pb
- n/p ratio of FAST, pre-equilibrium nucleons
- <u>Isospin fractionation and isoscaling in nuclear multifragmentation</u>
- <u>Isospin diffusion/transport</u>
- Neutron-proton differential flow
- Neutron-proton correlation functions at low relative momenta
- t/3He ratio
- Hard photon production
- Pigmy/Giant resonances
- Nucleon optical potential

Towards high densities reachable at CSR/Lanzhou, FAIR/GSI, RIKEN,

GANIL and, FRIB/MSU (高密度行为)

- π^{-}/π^{+} ratio, K^{+}/K^{0} ratio?
- Neutron-proton differential transverse flow
- n/p ratio at mid-rapidity
- Nucleon elliptical flow at high transverse momenta
- n/p ratio of squeeze-out emission

Nskin is an golden probe of Esym around nuclear saturation density!

B.A. Brown, PRL85, 5296 (2000) (Citations: 801+)

S. Typel/B.A. Brown, PRC64, 027302 (2000) (Citations: 303+)

R.J. Furnstahl, NPA706, 85 (2002) (Citations: 408+)

LWC/Ko/Li, PRC72, 064309 (2005) (Citations: 300+)

M. Centelles et al., PRL102, 122502 (2009) (Citations: 506+)

LWC/Ko/Li/Xu, PRC82, 024321 (2010) (Citations: 314+)

Zhang(张振)/LWC, PLB726, 234 (2013) (Citations: 205+)

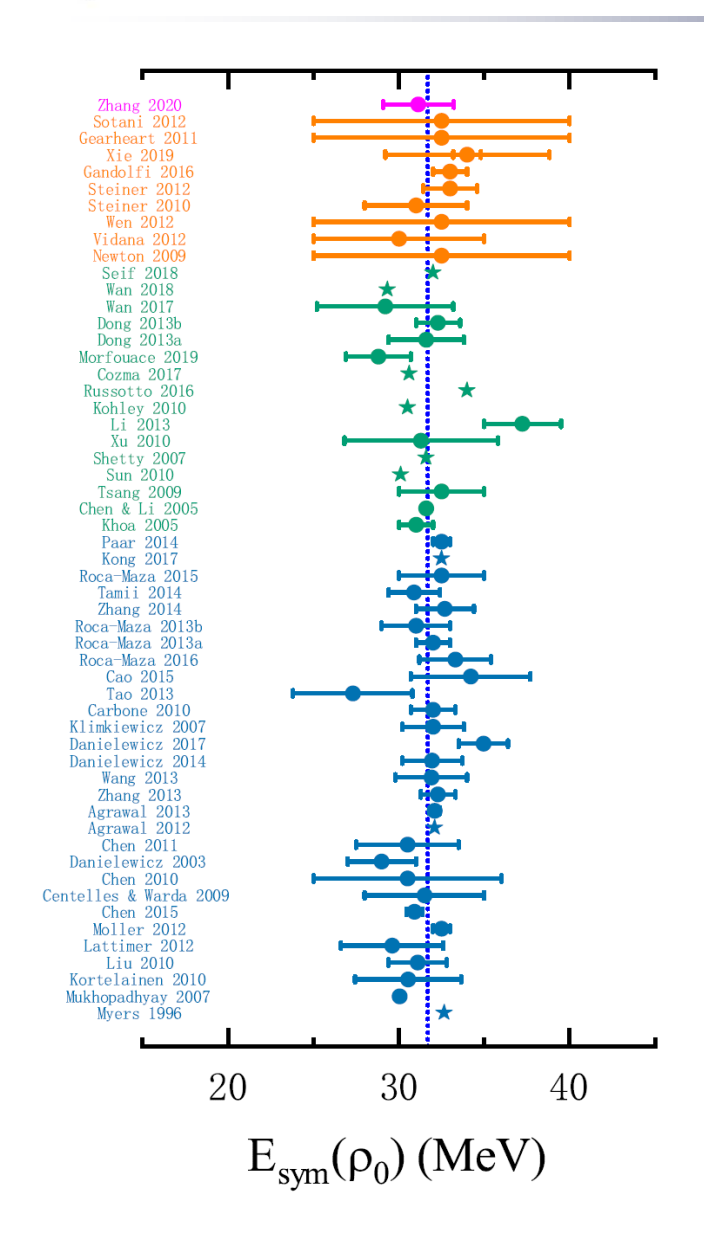
B.A. Li, LWC, C.M. Ko

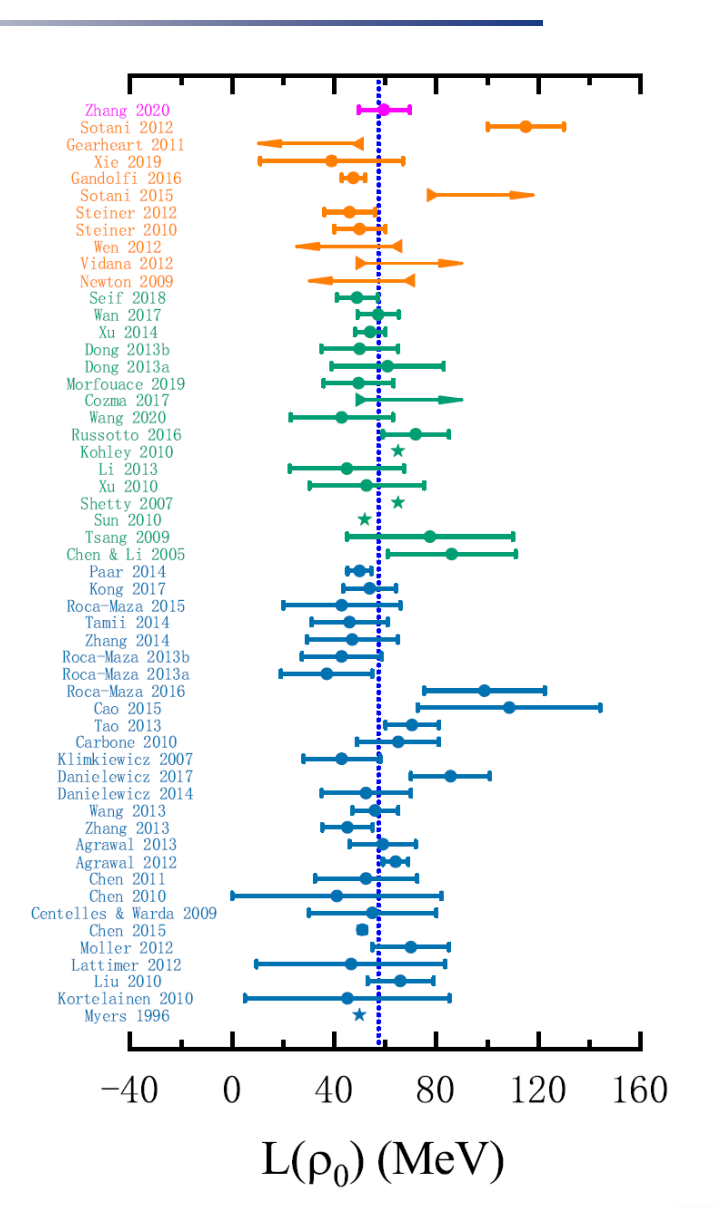
Phys. Rep. 464, 113(2008)

[arXiv:0804.3580] (Citations: 1336+)



E_{sym}: Around saturation density





LWC et al., Invited Review
58 analyses of terrestrial nuclear
experiments and astrophysical
observations

$$E_{\text{sym}}(\rho_0) = 31.7 \pm 3.1$$

 $L = 57.5 \pm 24.5 \text{ MeV}$

Similar conclusion has been obtained in:

- ◆ B. A. Li and X. Han, Phys. Lett. B727, 276 (2013);
- M. Oertel, M. Hempel, T. Klahn, and S. Typel, Rev. Mod. Phys. 89, 015007 (2017).



Assuming all the constraints are equally reliable !!!

Very recent PREX-II/CREX data suggest stiff/soft Esym around saturation density, and strong tension is observed!



Outline

Summary and outlook

The Symmetry Energy (Esym)
 Neutron Skin (Nskin): CREX/PREX puzzle
 Isovector Spin-Orbit Interaction

Neutron Skin

M. Thiel et al., JPG46, 093003 (2019)

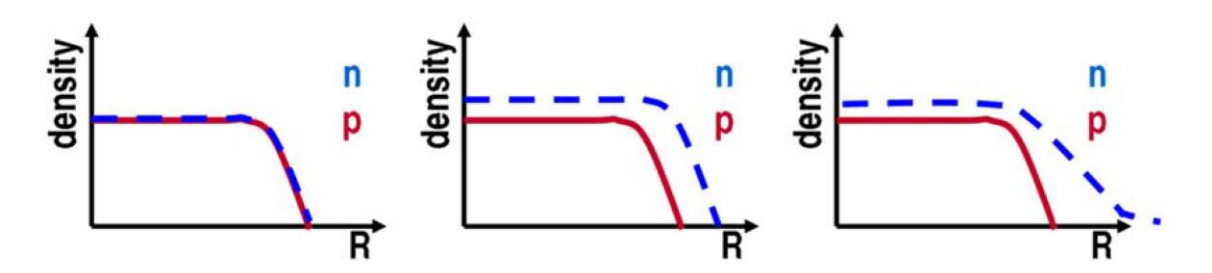


Figure 1. Schematic representation of charge and neutron density distributions. *Left:* Symmetric nuclear matter (N = Z) where $c_n \cong c_p$ and $a_n \cong a_p$. *Middle:* Asymmetric nuclear matter $(N \gg Z)$ having a neutron skin: $c_n > c_p$ and $a_n \cong a_p$. *Right:* Asymmetric nuclear matter $(N \gg Z)$ with a halo-type structure: $c_n > c_p$ and $a_n > a_p$.

$$\rho(r) = \frac{\rho_0}{1 + \exp[(r-c)/a]}$$

 ρ_0 : "Central" density; c: Half-density radius; a: Surface diffusion parameter

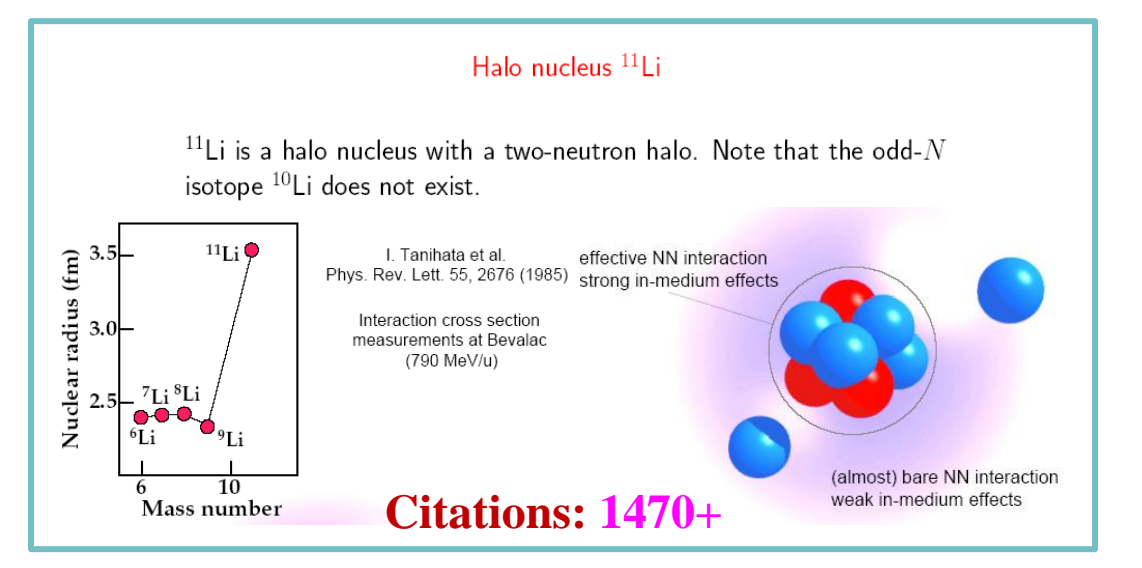
Neutron skin

$$R_{\rm skin} = R_n - R_p$$

 R_n : (point) neutron rms radius

 R_p : (point) proton rms radius

Halo nuclei





Neutron Skin

Nskin Data Tables

-0.7-0.7-0.7

-1.3-1.2

0.7

0.0

-1.00.4

TABLE I. Experimental and evaluated neutron skin thicknesses σ_I , AA, GDR, SDR, and PDR denote the interaction cross section, antiprotonic atom, giant dipole resonance, spin dipole resonance, and

pygmy dipole resonance, respectively.				TABLE I. (Continued.)					TABLE I. (Continued.)		ued.)		
	Experimental $\Delta r_{np}^{\rm exp}$ (fm)	Method	Evaluated Δr_{np}^{eva} (fm)	Difference $\frac{\Delta r_{np}^{eva} - \Delta r_{np}^{exp}}{\text{error}}$		Experimental $\Delta r_{np}^{\text{exp}}$ (fm)	Method	Evaluated Δr_{np}^{eva} (fm)	$\frac{\text{Difference}}{\frac{\Delta r_{np}^{eva} - \Delta r_{np}^{exp}}{\text{error}}}$		Experimental $\Delta r_{np}^{\rm exp}$ (fm)	Method	Evaluated Δr_{np}^{eva} (fm)
⁴⁰ Ca	-0.080(1000) [21,36]	AA	0.007(13)	0.1		0.210(50) [56]	(p, p)		-0.4		0.230(90) [49]	(α, α)	
Cu	0.020(30) [31]	(p, p)	0.007(13)	-0.4		0.230(50) [57]	(p, p)		-0.8		0.250(200) [64]	(p, p)	
	-0.070(120) [49]	(ρ, ρ) (α, α)		0.6		0.180(80) [58]	(p, p)		0.1		0.180(60) [70]	SDR	
	-0.016(50) [50]	(α, α)		0.5		0.160(100) [59]	(p, p)		0.3	¹²² Sn	0.146(16) [6]	(p, p)	0.151(15)
	-0.009(140) [51]			0.1		0.220(110) [60]	(p, p)		-0.3		0.220(70) [70]	SDR	
		(α, α)				0.168(55) [61]	(p, p)		0.4		0.200(90) [73]	(α, α)	
	-0.009(40) [52]	(α, α)		0.4		0.146(60) [29,62]	σ_l		0.8	124Sn	0.185(17) [6]	(p, p)	0.183(13)
	0.010(140) [53]	(p, p)		0.0	⁵⁸ Ni	-0.090(160) [21,36]	AA	-0.008(17)	0.5		0.140(30) [21,36]	AA	
	0.000(60) [54]	(p, p)		0.1		-0.010(30) [31]	(p, p)		0.1		0.160(90) [49]	(α, α)	
	0.014(30) [55]	(p, p)		-0.2		0.010(100) [49]	(α, α)		-0.2		0.250(50) [57]	(p, p)	
	-0.070(50) [56]	(p, p)		1.5		-0.097(137)[51]	(α, α)		0.6		0.220(70) [67]	(p, p)	
	0.100(50) [57]	(p, p)		-1.9		0.010(50) [57]	(p, p)		-0.4		0.190(70) [70]	SDR	
	0.010(80) [58]	(p, p)		0.0		0.030(120) [63]	(α, α)		-0.3		0.200(60) [71]	(p, p)	
	-0.010(100) [59]	(p, p)		0.2		0.180(200) [64]	(p, p)		-0.9		0.210(110) [72]	GDR	
	0.030(50) [60]	(p, p)		-0.5		0.010(80) [65]	(p, p)		-0.2	²⁰⁴ Pb	0.220(90) [74]	(α, α)	0.191(49)
	-0.010(49) [61]	(p, p)		0.3		-0.011(30) [66]	(p, p)		0.1		0.178(59) [75]	(p, p)	
⁴² Ca	0.080(30) [31]	(p, p)	0.055(16)	-0.8		-0.036(70) [67]	(p, p)		0.4	²⁰⁶ Pb	0.190(90) [74]	(α, α)	0.182(34)
	0.043(47) [50]	(α, α)	0.000(10)	0.3		-0.010(100) [68]	(p, p)		0.0		0.180(64) [75]	(p,p)	
	-0.030(134) [51]	(α, α)		0.6		0.096(248) [69]	(p, p)		-0.4		0.181(45) [76]	(p,p)	
	0.027(38) [52]	(α, α)		0.7	⁶⁰ Ni	-0.010(150) [21,36]	AA	-0.011(58)	0.0	²⁰⁸ Pb	0.150(20) [21,36]	AA	0.167(11)
	0.055(30) [55]			0.0		0.080(100) [49]	(α, α)		-0.9	10	0.250(90) [49]	(α, α)	0.107(11)
	0.080(80) [58]	(p, p)		-0.3		-0.051(132)[51]	(α, α)		0.3		0.080(50) [56]	(p,p)	
		(p, p)		0.0		-0.080(100) [68]	(p, p)		0.7		0.160(50) [57]	(p,p)	
	0.060(130) [60]	(p, p)			⁶² Ni	0.090(100) [49]	(α, α)	0.075(62)	-0.2		0.060(100) [59]	(p,p)	
	0.049(60) [29,62]	σ_{l}		0.1		0.044(127) [51]	(α, α)		0.2		0.360(200) [64]	(p,p)	
⁴⁴ Ca	0.130(30) [31]	(p, p)	0.091(15)	-1.3		0.080(100) [68]	(p, p)		-0.1		0.180(70) [67]	(p,p)	
	0.090(160) [49]	(α, α)		0.0	⁶⁴ Ni	0.040(80) [21,36]	AA	0.129(34)	1.1		0.190(90) [72]	GDR	
	0.079(45) [50]	(α, α)		0.3		0.100(123) [51]	(α, α)		0.2		0.300(70) [74]	(α, α)	
	-0.011(129) [51]	(α, α)		0.8		0.170(50) [57]	(p, p)		-0.8		0.211(63) [75]	(p, p)	
	0.044(36) [52]	(α, α)		1.3		0.180(80) [65]	(p, p)		-0.6		0.197(42) [76]	(p, p)	
	-0.020(120) [53]	(p, p)		0.9		0.040(100) [68]	(p, p)		0.9		0.260(130) [77]	(α, α)	
	0.088(30) [55]	(p, p)		0.1	112Sn	0.070(20) [21,36]	AA	0.070(20)	0.0		0.420(200) [77]	(α, α)	
	0.100(80) [58]	(p,p)		-0.1	114Sn	0.040(50) [70]	SDR	0.040(50)	0.0		0.273(90) [78]	(α, α)	
	0.110(170) [60]	(p,p)		-0.1	116Sn	0.110(18) [6]	(p, p)	0.111(13)	0.1		0.182(70) [79]	(p, p)	
	0.125(50) [29,62]	σ_{I}		-0.7		0.100(30) [21,36]	AA	()	0.4		0.140(40) [80]	(p, p)	
46.0			0.151(50)			0.080(90) [49]	(α, α)		0.3		0.180(35) [81]	PDR	
⁴⁶ Ca	0.151(50) [29,62]	σ_{l}	0.151(50)	0.0		0.150(50) [57]	(p, p)		-0.8		0.120(70) [82]	GDR	
⁴⁸ Ca	0.090(50) [21,36]	AA	0.191(13)	2.0		0.130(70) [67]	(p,p)		-0.3		0.160(45) [83]	AA	
	0.210(30) [31]	(p, p)		-0.6		0.120(60) [70]	SDR		-0.2		0.200(64) [32]	AA	
	0.330(120) [49]	(α, α)		-1.2		0.120(60) [71]	(p, p)		-0.2	106 Cd	0.100(140) [21,36]	AA	0.100(140)
	0.196(42) [50]	(α, α)		-0.1		0.020(120) [72]	GDR		0.8	110 Cd	0.076(14) [33]	(α, α)	0.076(14)
	0.096(119) [51]	(α, α)		0.8	118Sn	0.145(16) [6]	(p, p)	0.145(15)	0.0	¹¹² Cd	0.074(14) [33]	(α, α)	0.074(14)
	0.214(50) [52]	(α, α)		-0.5		0.170(90) [49]	(α, α)	()	-0.3	114Cd			
	0.390(100) [53]	(p, p)		-2.0		0.130(60) [70]	SDR		0.3		0.090(15) [33]	(α, α)	0.090(15)
	0.130(60) [54]	(p,p)		1.0	120Sn	0.147(33) [6]	(p, p)	0.137(23)	-0.3	¹¹⁶ Cd	0.150(40) [21,36]	AA	0.111(14)
	0.190(30) [55]	(p,p)		0.0	SII	0.080(40) [21,36]	AA	0.157(23)	1.4		0.105(15) [33]	(α, α)	

J.T. Zhang, X.L. Tu, P. Sarriguren, K. Yue et al., PRC104, 034303 (2021)

Nskin of Ca, Ni, Sn, Pb, Cd:

1. σ_{I} : Interaction cross section

2. AA: Antiprotonic atom

3. GDR: Giant dipole resonance

4. SDR: Spin dipole resonance

5. PDR: Pygmy dipole resonance

See also a Recent Review of Nskin:

M. Q. Ding, D.Q. Fang and Y.G. Ma, NST35, 211 (2024) [arXiv:2409.07059]

While Rc can be determined with high precision, the high precision determination of neutron rms radius (Nskin) remains a big challenge, even for stable nuclei!



NSkin: Model Dependence

The R_n (Rskin): usually determined from strong processes, generally involved in significant model dependence!

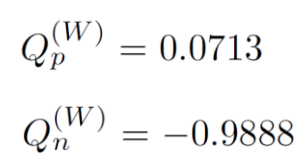
Clean/model-independent approaches to determine R_n (Rskin):

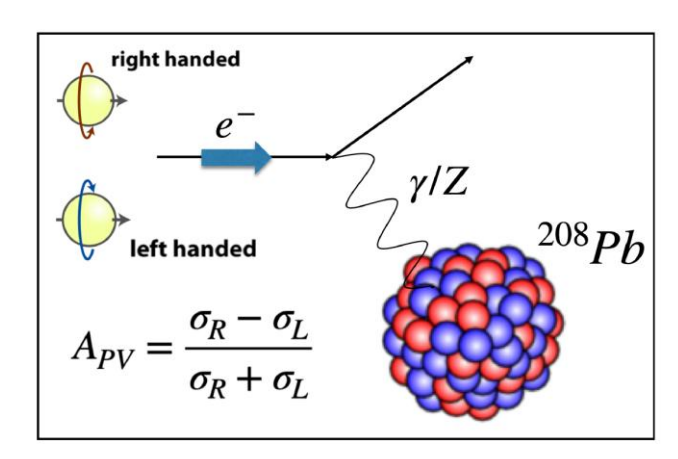
- PVES: Parity-violating asymmetry A_{PV} in the elastic scattering of polarized electrons from the nucleus since the A_{PV} is particularly sensitive to the neutron distribution due to its large weak charge compared to the tiny one of the proton (T.W. Donnelly et al., NPA503, 589 (1989); C.J. Horowitz et al., PRC63, 025501 (2001))
- Coherent elastic neutrino-nucleus scattering (CEvNS) (D. Z. Freedman, PRD 9, 1389 (1974); Spallation Neutron Source at Oak Ridge: D. Akimov et al. (COHERENT Collaboration), Science 357, 1123 (2017); M. Cadeddu, C. Giunti, Y. F. Li, and Y. Y. Zhang, PRL120, 072501 (2018); X.R. Huang/LWC, PRD 100, 071301 (2019); Supernova Neutrinos: X.R. Huang/LWC, PRD106, 123034(2022))

While the statistics of CEvNS data is too poor to claim a determination of Nskin, the PVES experiments have made significant progress!

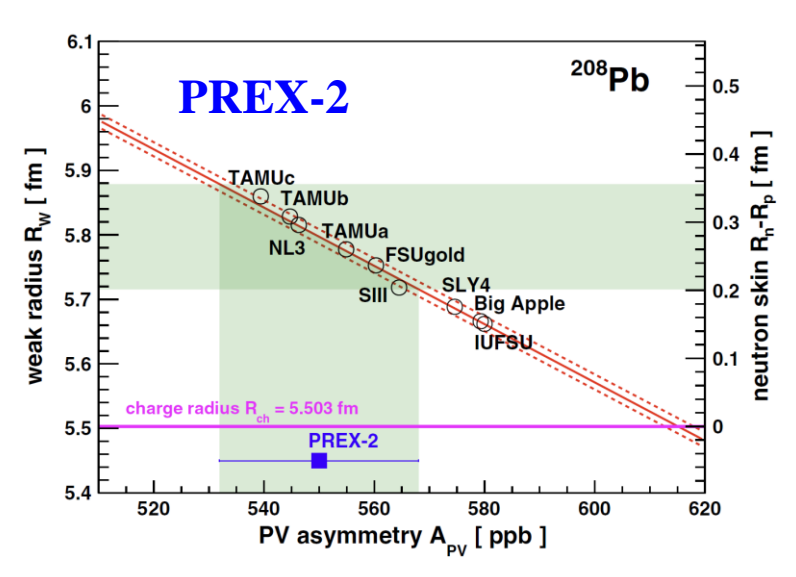


²⁰⁸Pb Radius EXperiment: PREX





PREX@JLab



Adhikari et al., PRL126, 172502 (2021)

■ Parity-violating asymmetry in longitudinally polarized elastic electron scattering :

$$A_{
m PV} = rac{\sigma_R - \sigma_L}{\sigma_R + \sigma_L} pprox rac{G_F Q^2 |Q_W|}{4\sqrt{2}\pilpha Z} rac{F_W(Q^2)}{F_{
m ch}(Q^2)}$$

T.W. Donnelly et al., NPA503, 589 (1989); C.J. Horowitz et al., PRC63, 025501 (2001).

- **□** Free from most strong interaction uncertainties.
- \square PREX-2 results ($\langle Q^2 \rangle = 0.00616 \text{ GeV}^2$):

$$A_{
m PV}^{
m meas} = 550 \pm 16 ({
m \ stat}\) \pm 8 ({
m \ syst}\) {
m ppb} \ F_Wig(ig\langle Q^2ig
angleig) = 0.368 \pm 0.013 ({
m exp}) \pm 0.001 ({
m \ theo}\)$$

²⁰⁸ Pb Parameter	Value
Weak radius (R_W) Interior weak density (ρ_W^0) Interior baryon density (ρ_b^0)	$5.800 \pm 0.075 \text{ fm}$ $-0.0796 \pm 0.0038 \text{ fm}^{-3}$ $0.1480 \pm 0.0038 \text{ fm}^{-3}$
Neutron skin $(R_n - R_p)$	$0.283 \pm 0.071 \text{ fm}$



⁴⁸Ca Radius EXperiment: CREX

CREX, PRL129, 042501 (2022)

PHYSICAL REVIEW LETTERS 129, 042501 (2022)

Editors' Suggestion

Precision Determination of the Neutral Weak Form Factor of ⁴⁸Ca

■ Model-independent determination of charge-weak form factor difference:

$$\Delta F_{
m CW}^{48}(q)\!=\!0.0277\pm0.0055$$
 , $q=~0.8733~{
m fm}^{-1}$ CREX

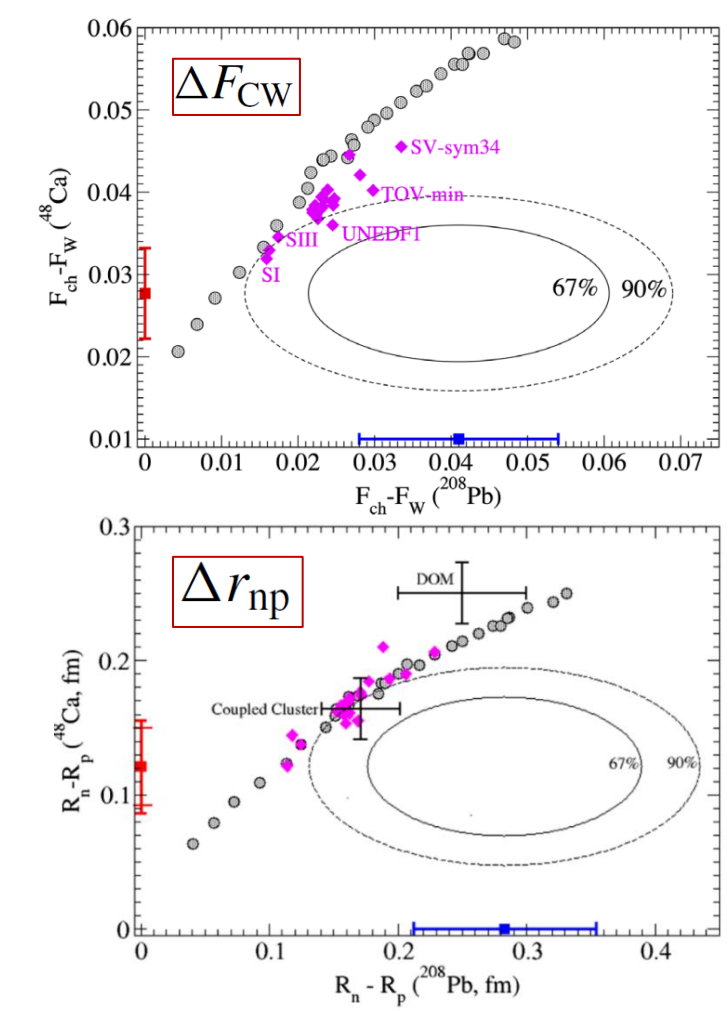
$$\Delta F_{\rm CW}^{208}(q) = 0.041 \pm 0.013, \ q = 0.3977 \ {
m fm}^{-1}$$
 PREX-2

■ Extracted neutron skin of Ca48

Quantity	$Value \pm (exp) \pm (model) (fm)$
$R_W - R_{\rm ch} \\ R_n - R_p$	$0.159 \pm 0.026 \pm 0.023$ $0.121 \pm 0.026 \pm 0.024$

☐ Strong tension between CREX and PREX-2 results?

Too small Nskin in ⁴⁸Ca or too large Nskin in ²⁰⁸Pb



Challenging modern nuclear EDF theory! "PREX-CREX Puzzle (Pb/Ca中子半径之谜)"

See also: Reinhard/Roca-Maza/Nazarewicz, PRL129, 042501 (2022)



PREX and CREX: A Bayesian analysis

SHF

base data of nuclei

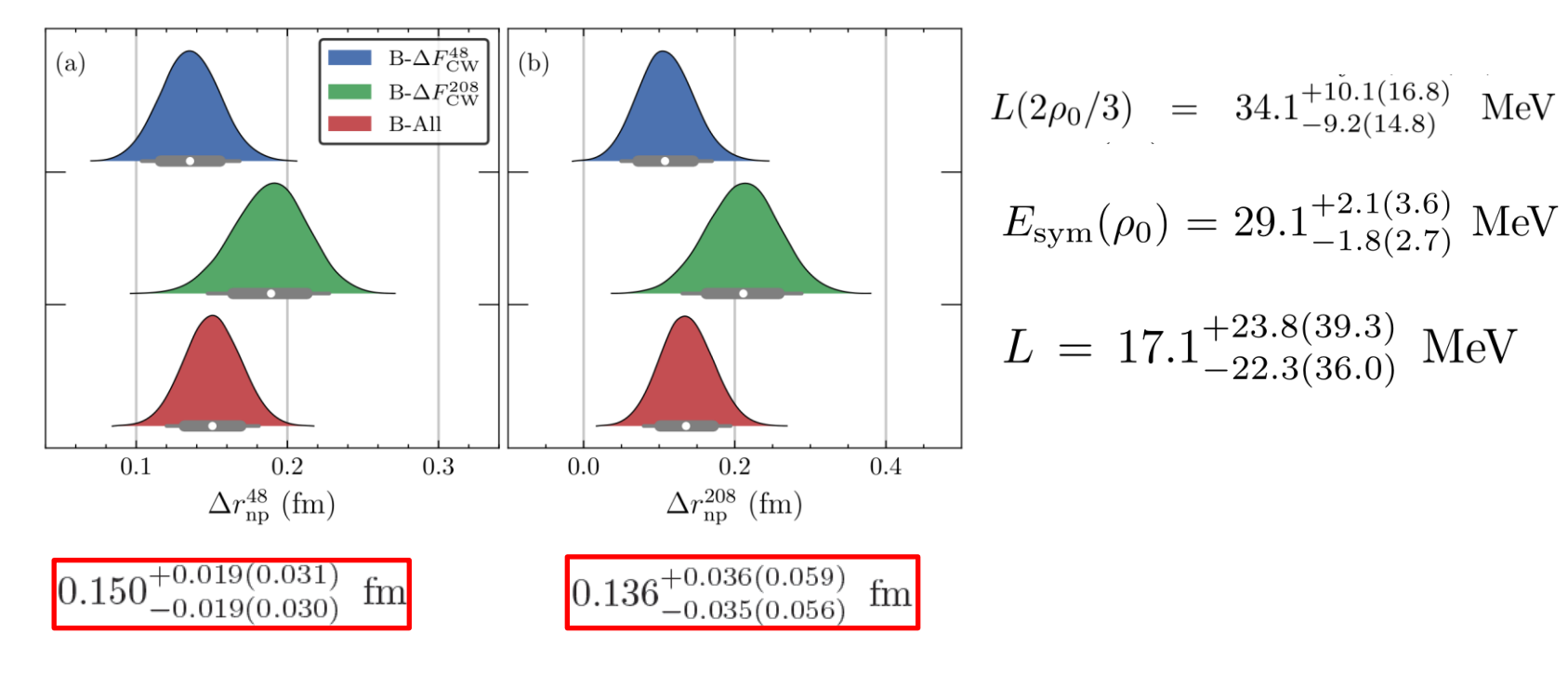
TABLE II. Experimental data and adopted errors used in the Bayesian analysis. The second line shows the globally adopted error for each observable. That error is multiplied for each observable by a further integer weight factor given in the parenthesis next to the data value.

Nuclei	$E_{ m B}$	r_c	R_d	σ	$\Delta\epsilon_{ls}$
	(1 MeV)	(0.02 fm)	(0.04 fm)	(0.04 fm)	(20%)
¹⁶ O	-127.620(4)	2.701(2)	2.777(2)	0.839(2)	6.30(3)
					6.10(3)
$^{40}\mathrm{Ca}$	-342.051(3)	3.478(1)	3.845(1)	0.978(1)	
$^{48}\mathrm{Ca}$	-415.990(1)	3.479(2)	3.964(1)	0.881(1)	
	-483.990(5)	3.750(9)			
$^{68}\mathrm{Ni}$	-590.430(1)				
$^{100}\mathrm{Sn}$	-825.800(2)				
$^{132}\mathrm{Sn}$	-1102.900(1)				1.35(1)
	` /				1.65(1)
$^{208}\mathrm{Pb}$	-1636.446(1)	5.504(1)	6.776(1)	0.913(1)	1.32(1)
	` /	()	()	` /	0.90(1)
					1.77(2)

Note. $\Delta \epsilon_{ls}$ data are for $^{16}\text{O}(1p_p, 1p_n)$, $^{132}\text{Sn}(2p_p, 2d_n)$, and $^{208}\text{Pb}(2d_p, 3p_n, 2f_n)$, respectively.

Also n-p Fermi energy difference of ¹⁶O, ^{40,48}Ca, ⁵⁶Ni, ¹³²Sn, ²⁰⁸Pb and GMR of ²⁰⁸Pb

Zhang/Chen, PRC108, 024317 (2023) [arXiv: 2207.03328]



- □ CREX and PREX are (in)compatible in (68)90% C.L.
- **□** PREX is less effective to constrain Esym due to its lower precision compared to CREX
- □ Combining CREX+PREX favors mildly soft Esym around saturation density!

α-Clustering effects? S. Yang, R.J. Li, and C. Xu, PRC108, L021303 (2023)
Symmetry energy? Reed, Fattoyev, Horowitz, and Piekarewicz, PRC 109, 035803 (2024)



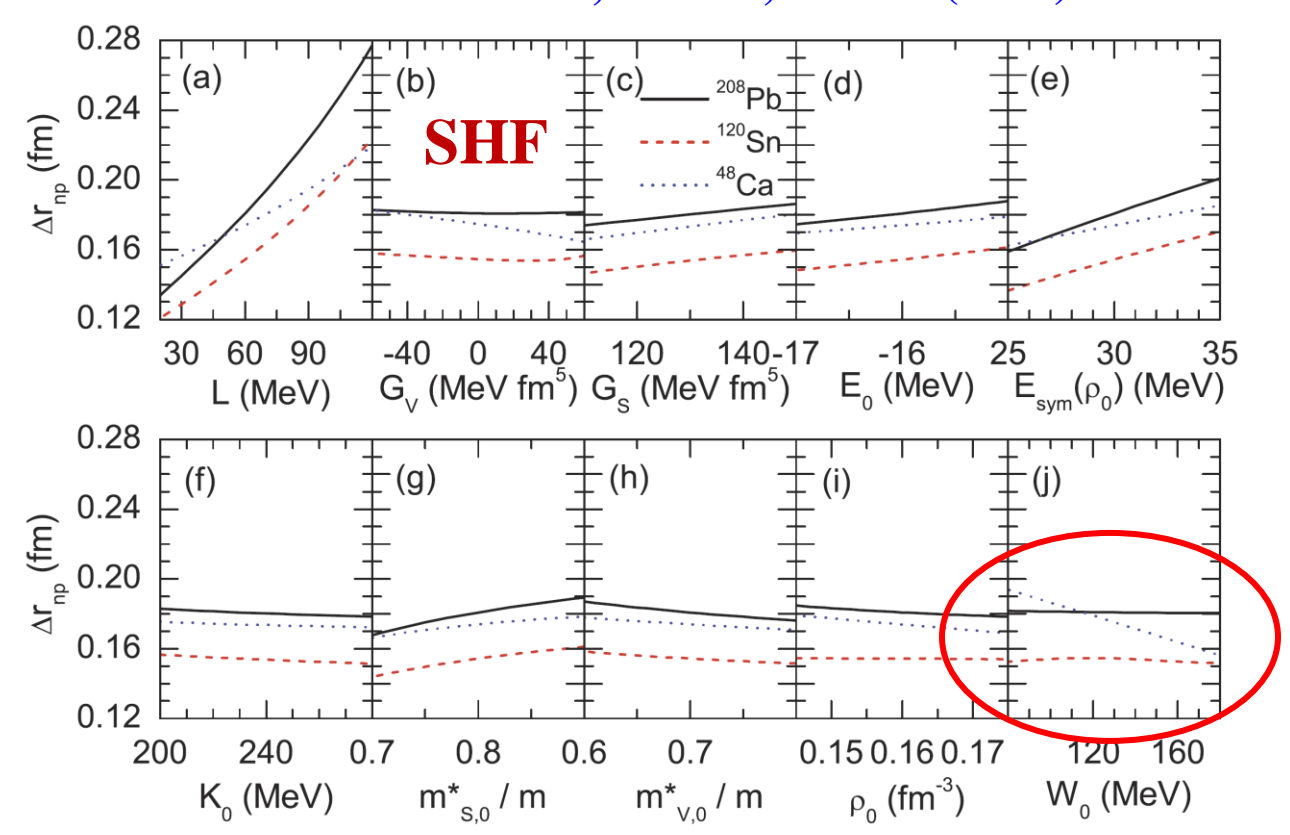
Outline

- ☐ The Symmetry Energy (Esym)
- Neutron Skin (Nskin): CREX/PREX puzzle
- Isovector Spin-Orbit Interaction
- ☐ Summary and outlook



NSkin vs Spin-Orbit Interaction

LWC/Ko/Li/Xu, PRC82, 024321 (2010)



Horowitz/Piekarewitz, PRC86, 045503 (2012)

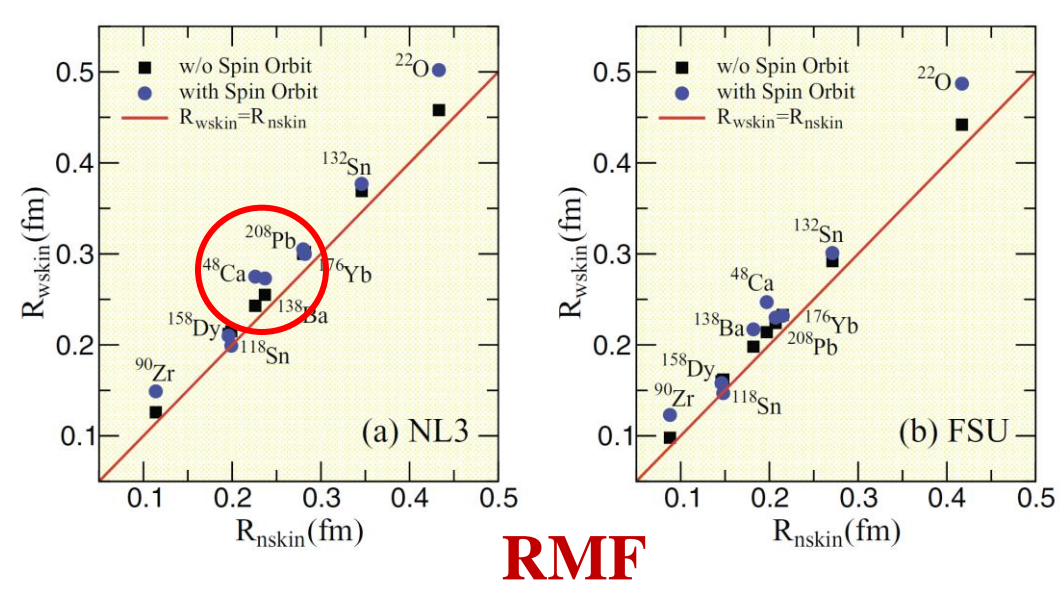
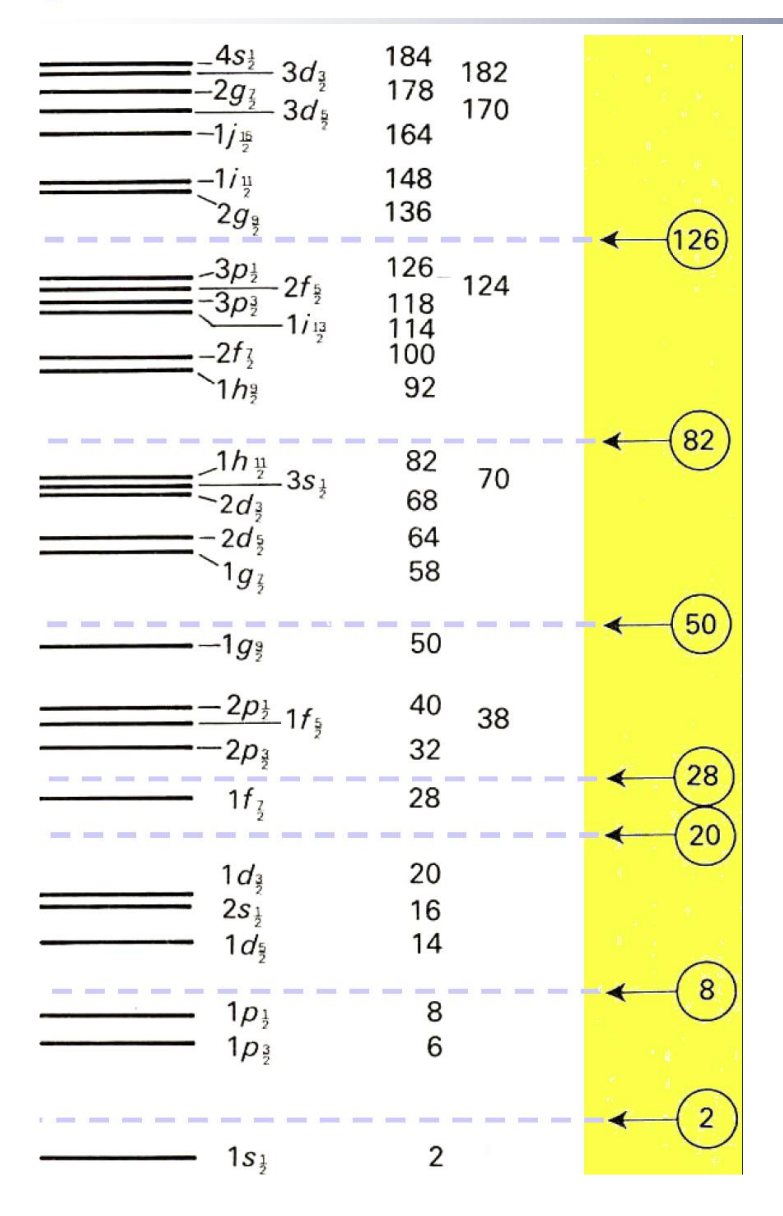


FIG. 2. (Color online) Electroweak skin $(R_{\rm wk}-R_{\rm ch})$ with and without spin-orbit corrections as a function of neutron skin (R_n-R_p) for the various neutron-rich nuclei considered in this work. Predictions are made using both the (a) NL3 and (b) FSU interactions.

- **■** The Nskin of Ca48 is sensitive to spin-orbit coupling W0 in the standard SHF!
- **□** Spin-orbit coupling makes significant contribution to Rwk-Rch
- □ Ca48 and Pb208 have different shell and surface structures Both are related to Spin-Orbit interaction





Nuclear Magic Numbers: Strong Spin-Orbit (l•s) Interaction

$$V(r) \to V(r) + W(r)L \cdot S$$

$$W(r) = -|V_{LS}| \left(\frac{\hbar}{m_{\pi}c}\right)^{2} \frac{1}{r} \frac{dV(r)}{dr}$$



Mayer and Jensen (1949) Nobel Prize, 1963 (Also Wigner)

Relativistic effects (Duerr, PR103, 469(1956))

- **□** Strong SO interaction naturally appears in RMF
- Nonrelativistic energy density functionals (e.g., Skyrme)

Spin-orbit interaction: $iW_0 \sigma \cdot [P' \times \delta(r)P]$

Spin-orbit energy density:

$$\mathcal{H}_{\text{so}} = \frac{1}{2} W_0 \left[J \cdot \nabla \rho + J_p \nabla \rho_p + J_n \nabla_n \right]$$

☐ Is the SO interaction of neutrons significantly different from that of protons?

上海交通大學 SHANGHAI JIAO TONG UNIVERSITY CREX/PREX: Strong Isovector Spin-Orbit Interaction

☐ Hamiltonian Density from Spin-Orbit Interaction:

$$E_{\rm so} = \int d^3r \left[\frac{b_{\rm IS}}{2} \boldsymbol{J} \cdot \boldsymbol{\nabla} \rho + \frac{b_{\rm IV}}{2} (\boldsymbol{J}_n - \boldsymbol{J}_p) \cdot \boldsymbol{\nabla} (\rho_n - \rho_p) \right]$$
 Sharma, Lalazissis, Konig, and Ring, PRL 74, 3744 (1995). Reinhard and Flocard, NPA 584, 467488 (1995). ISOvector

■ Standard Skyrme EDF:

$$b_{\rm IV} = b_{\rm IS}/3 = W_0/2 \approx 60 \ {\rm MeV \cdot fm}^5$$

Reinhard and Flocard, NPA 584, 467488 (1995); Bender, Heenen, and Reinhard, Rev. Mod. Phys. 75, 121 (2003).

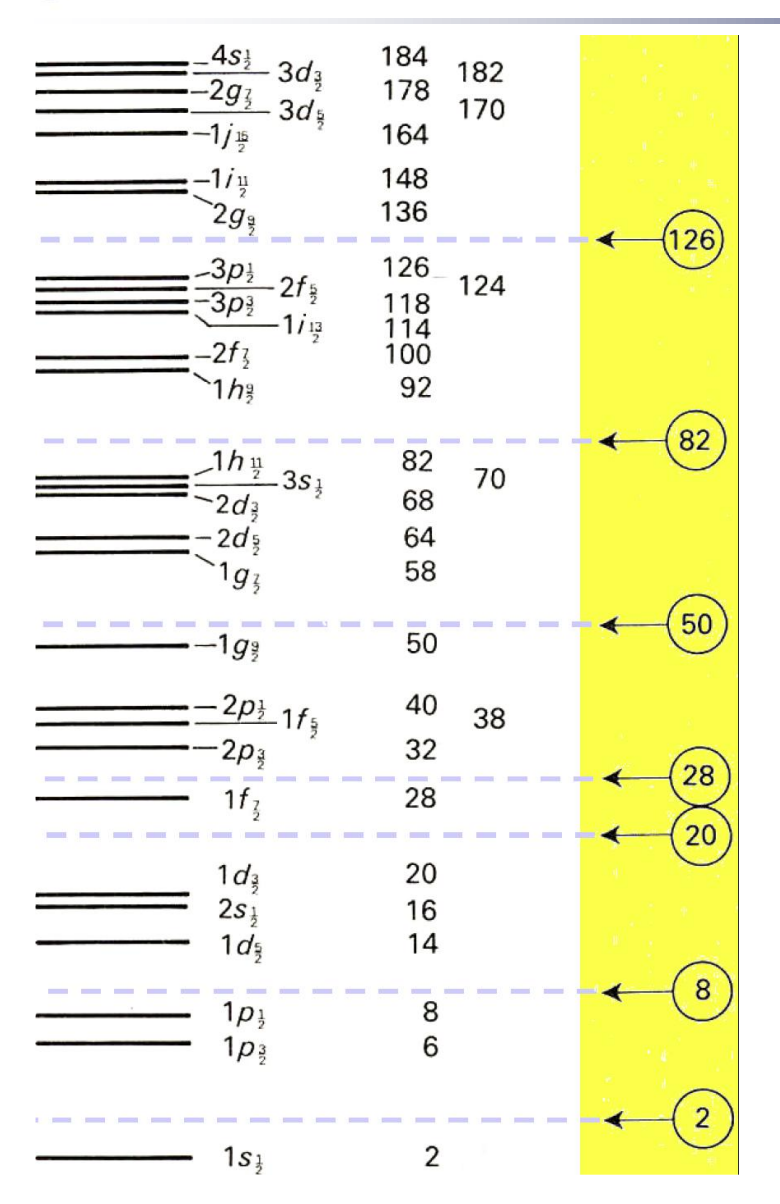
Conventional relativistic mean field model (nonrelativistic reduction):

$$b_{\rm IV} \approx 0$$

Ebran, Mutschler, Khan, and Vretenar, PRC 94, 024304 (2016).

- \square Lack of experimental probes to constrain b_{IV}
- The isovector spin-orbit coupling b_{1V} is expected to have significant effects on lighter nuclear with larger $J_n - J_p$.





□ Spin-Orbit density:

$$J_{q}(r) = \frac{1}{4\pi r^{3}} \sum_{i} v_{i}^{2} (2j_{i} + 1)$$

$$\times \left[j_{i} (j_{i} + 1) - l_{i} (l_{i} + 1) - \frac{3}{4} \right] R_{i}^{2}(r)$$
208Pb

 \Box Jq ~ 0 for spin-saturated nuclei:

Both $j_> = l+1/2$ and $j_< = l-1/2$ are fully occupied, and $j_>$ (positive) and $j_<$ (negative) largely cancel each other out

Ca40: $Jn \approx 0$, $Jp \approx 0$

Ca48: $Jp \approx 0$, Jn >> 0 due to the 8 1f7/2 neutrons of unpaired l•s partner

Pb208: Jn \approx Jp >> 0 due to 14 1i13/2 neutrons and 12 1h11/2 protons

So Jn - Jp >> 0 for Ca48 while Jn - Jp ≈ 0 for Pb208:

Therefore, the isovector spin-orbit coupling \mathbf{b}_{IV} is expected to have significant effect on Ca48 while essentially no influence on Pb208!

Jn

Jp



Extended Skyrme EDF with tensor force

□ Standard Skyrme interaction:

$$\begin{split} v\left(r_{1},r_{2}\right) &= t_{0}\left(1+x_{0}P_{\sigma}\right)\delta(\mathbf{r}) + \frac{1}{2}t_{1}\left(1+x_{1}P_{\sigma}\right)\left[\mathbf{k}'^{2}\delta(\mathbf{r})+\delta(\mathbf{r})\mathbf{k}^{2}\right] + t_{2}\left(1+x_{2}P_{\sigma}\right)\mathbf{k}'\cdot\delta(\mathbf{r})\mathbf{k} \\ &+ \frac{1}{6}t_{3}\left(1+x_{3}P_{\sigma}\right)\left[\rho(\mathbf{R})\right]^{\alpha}\delta(\mathbf{r}) + iW_{0}(\sigma_{1}+\sigma_{2})\cdot\left[\mathbf{k}'\times\delta(\mathbf{r})\mathbf{k}\right], \end{split} \qquad \begin{array}{l} \text{D. Vautherin and D. M. Brink, PRC5, 626 (1972);} \\ \text{D. Vautherin, PRC7, 296 (1973)} \\ \text{E. Chabanat, et al., NPA 627, 710 (1997);} \end{split}$$

■ Momentum-dependent many-body interaction:

$$v' = v + \frac{1}{2}t_4\left(1 + x_4P_\sigma\right)\left[\mathbf{k}'^2\rho(R)^\beta\delta(\mathbf{r}) + \delta(\mathbf{r})\rho(R)^\beta\mathbf{k}^2\right] + t_5\left(1 + x_5P_\sigma\right)\mathbf{k}' \cdot \rho(R)^\gamma\delta(\mathbf{r})\mathbf{k}.$$

N. Chamel, S. Goriely, and J.M. Pearson, PRC80, 065804 (2009)

Zhang & Chen, PRC 94, 064326 (2016)

NPA 635, 231 (1998)

□ Zero-range tensor force:

$$V_{T} = \frac{1}{2}T\left\{ \left[\left(\sigma_{1} \cdot \mathbf{k}'\right)\left(\sigma_{2} \cdot \mathbf{k}'\right) - \frac{1}{3}\mathbf{k}'^{2}\left(\sigma_{1} \cdot \sigma_{2}\right) \right] \delta\left(\mathbf{r}\right) + \delta\left(\mathbf{r}\right) \left[\left(\sigma_{1} \cdot \mathbf{k}\right)\left(\sigma_{2} \cdot \mathbf{k}\right) - \frac{1}{3}\mathbf{k}^{2}\left(\sigma_{1} \cdot \sigma_{2}\right) \right] \right\} + U\left\{ \left(\sigma_{1} \cdot \mathbf{k}'\right) \delta\left(\mathbf{r}\right)\left(\sigma_{2} \cdot \mathbf{k}\right) - \frac{1}{3}\left(\sigma_{1} \cdot \sigma_{2}\right) \left[\mathbf{k}' \cdot \delta\left(\mathbf{r}\right)\mathbf{k}\right] \right\},$$

$$\mathbf{Stancu, Brink, and Flocard, PLB 68, 108 (1977)}$$



上海交通大學 SHANGHAI JIAO TONG UNIVERSITY Extended Skyrme EDF with tensor force

Energy density functional:

$$\begin{split} \mathcal{E}_{\text{Skyrme}} \; &= \; \frac{B_0 + B_3 \rho^\alpha}{2} \rho^2 - \frac{B_0' + B_3' \rho^\alpha}{2} \tilde{\rho}^2 + (B_1 + B_4 \rho^\beta + B_5 \rho^\gamma) \rho \tau - (B_1' + B_4' \rho^\beta + B_5' \rho^\gamma) \tilde{\rho} \tilde{\tau} \\ &+ \frac{2B_2 + (2\beta + 3)B_4 \rho^\beta - B_5 \rho^\gamma}{4} (\nabla \rho)^2 - \frac{2B_2' + 3B_4' \rho^\beta - B_5' \rho^\gamma}{4} (\nabla \tilde{\rho})^2 - \frac{\beta B_4'}{2} \rho^{\beta - 1} \tilde{\rho} \nabla \rho \cdot \nabla \tilde{\rho} \\ &+ \frac{C_1 + C_2 \rho^\beta + C_3 \rho^\gamma}{2} J^2 + \frac{C_1' + C_2' \rho^\beta + C_3' \rho^\gamma}{2} \tilde{J}^2 \\ &+ \frac{b_{\text{IS}}}{2} \nabla \rho \cdot \mathbf{J} + \frac{b_{\text{IV}}}{2} \nabla \tilde{\rho} \cdot \tilde{\mathbf{J}} + \frac{\alpha_T + \beta_T}{4} J^2 + \frac{\alpha_T - \beta_T}{4} \tilde{J}^2. \end{split}$$

$$\rho_{q}(\mathbf{r}) = \sum_{i} v_{i}^{2} |\varphi_{i}(\mathbf{r})|^{2},$$

$$\tau_{q}(\mathbf{r}) = \sum_{i} v_{i}^{2} |\nabla \varphi_{i}(\mathbf{r})|^{2},$$

$$\rho = \rho_{n} + \rho_{p}, \quad \tau = \tau_{n} + \tau_{p}, \quad J = J_{n} + J_{p},$$

$$\tilde{\rho} = \rho_{n} - \rho_{p}, \quad \tilde{\tau} = \tau_{n} - \tau_{p}, \quad \tilde{J} = J_{n} - J_{p},$$

$$J_{q}(\mathbf{r}) = -i \sum_{i} v_{i}^{2} \varphi_{i}^{+}(\mathbf{r}) \nabla \times \hat{\sigma} \varphi_{i}(\mathbf{r}).$$



Extended Skyrme EDF with tensor force

□ Nucleon mean-field Hamiltonian:

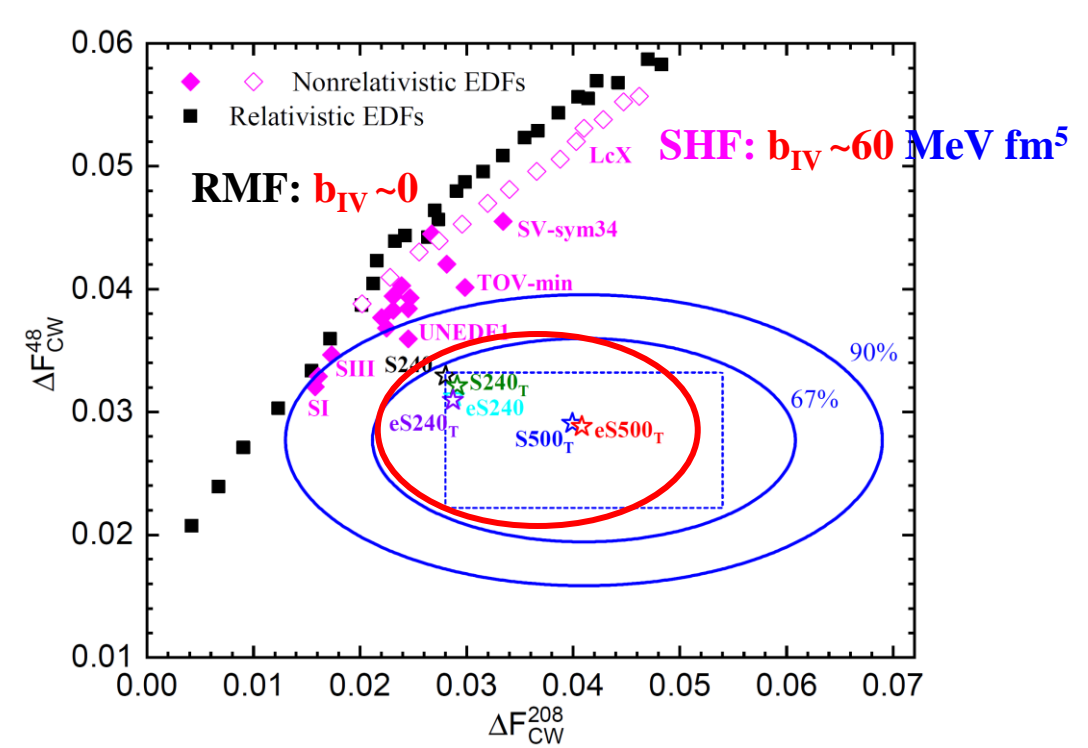
$$\begin{split} \hat{h}_{q} &= -\boldsymbol{\nabla} \cdot \frac{\hbar^{2}}{2m_{q}^{*}} \boldsymbol{\nabla} + \boldsymbol{U}_{q} + i\boldsymbol{W}_{q} \cdot (\boldsymbol{\sigma} \times \boldsymbol{\nabla}), \ \boldsymbol{q} = \boldsymbol{n}, \ \boldsymbol{p} \\ & \frac{\hbar^{2}}{2m_{q}^{*}} = \frac{\partial \mathcal{E}}{\partial \tau_{q}}, \ \boldsymbol{U}_{q} = \frac{\partial \mathcal{E}}{\partial \rho_{q}} - \boldsymbol{\nabla} \cdot \frac{\partial \mathcal{E}}{\partial \left[\boldsymbol{\nabla} \rho_{q}\right]}, \ \boldsymbol{W}_{q} = \frac{\partial \mathcal{E}}{\partial \boldsymbol{J}_{q}} \\ \boldsymbol{U}_{q} &= B_{0}\rho - t_{q}B_{0}'\tilde{\rho} + B_{1}\tau - t_{q}B_{1}'\tilde{\tau} + \frac{\alpha + 2}{2}B_{3}\rho^{\alpha + 1} - \frac{B_{3}'}{2}(\alpha\tilde{\rho} + 2t_{q}\rho)\rho^{\alpha - 1}\tilde{\rho} \\ & + (\beta + 1)B_{4}\rho^{\beta}\tau + (\gamma + 1)B_{5}\rho^{\gamma}\tau - (B_{4}'\beta\rho^{\beta} + B_{5}'\gamma\rho^{\gamma})\tilde{\rho}\tilde{\tau} - t_{q}(B_{1}' + B_{4}'\rho^{\beta} + B_{5}'\rho^{\gamma})\tilde{\tau} \\ & - \frac{\beta(2\beta + 3)B_{4}\rho^{\beta - 1} - B_{5}\gamma\rho^{\gamma - 1}}{4}(\boldsymbol{\nabla}\rho)^{2} - \frac{2B_{2} + (2\beta + 3)B_{4}\rho^{\beta} - B_{5}\rho^{\gamma}}{2}\boldsymbol{\nabla}^{2}\rho \\ & - \frac{3\beta B_{4}'\rho^{\beta - 1} - \gamma B_{5}'\rho^{\gamma - 1}}{4}\boldsymbol{\nabla}\tilde{\rho} \cdot (2t_{q}\boldsymbol{\nabla}\rho + \boldsymbol{\nabla}\tilde{\rho}) - \frac{2B_{2}' + 3B_{4}'\rho^{\beta} - B_{5}'\rho^{\gamma}}{2}t_{q}\boldsymbol{\nabla}^{2}\tilde{\rho} \\ & + \frac{\beta B_{4}'}{2}\rho^{\beta - 1}(\boldsymbol{\nabla}\tilde{\rho})^{2} + \frac{\beta B_{4}'}{2}\rho^{\beta - 1}\tilde{\rho}\boldsymbol{\nabla}^{2}\tilde{\rho} + \frac{\beta(\beta - 1)B_{4}'}{2}\rho^{\beta - 2}\tilde{\rho}(\boldsymbol{\nabla}\rho)^{2}t_{q} + \frac{\beta B_{4}'}{2}\rho^{\beta - 1}\tilde{\rho}(\boldsymbol{\nabla}^{2}\rho)t_{q} \\ & + \frac{\beta C_{2}\rho^{\beta - 1} + \gamma C_{3}\rho^{\gamma - 1}}{2}\boldsymbol{J}^{2} + \frac{\beta C_{2}'\rho^{\beta - 1} + \gamma C_{3}'\rho^{\gamma - 1}}{2}\boldsymbol{J}^{2} - \frac{b_{1S}}{2}\boldsymbol{\nabla}\cdot\boldsymbol{J} - t_{q}\frac{b_{1V}}{2}\boldsymbol{\nabla}\cdot\boldsymbol{J}, \end{split}$$

$$\boldsymbol{W}_{q} = \frac{b_{\mathrm{IS}}}{2} \nabla \rho + t_{q} \frac{b_{\mathrm{IV}}}{2} \nabla (\rho_{n} - \rho_{p}) + \frac{\alpha_{\mathrm{J}} + \beta_{\mathrm{J}}}{2} \boldsymbol{J} + t_{q} \frac{\alpha_{\mathrm{J}} - \beta_{\mathrm{J}}}{2} (\boldsymbol{J}_{n} - \boldsymbol{J}_{p})$$

Construct 6 new EDFs to simultaneously fit CREX and PREX results, ground- and excited-state of a number of typical (semi-)closed-shell nuclei, and constraints on EOS of nuclear matter. (e)S500T, (e)S240T, and (e)S240. [e: extended, T: tensor force, number: the value of b_{IV}]



Tong-Gang Yue/Zhen Zhang/CLW, arXiv:2406.03844



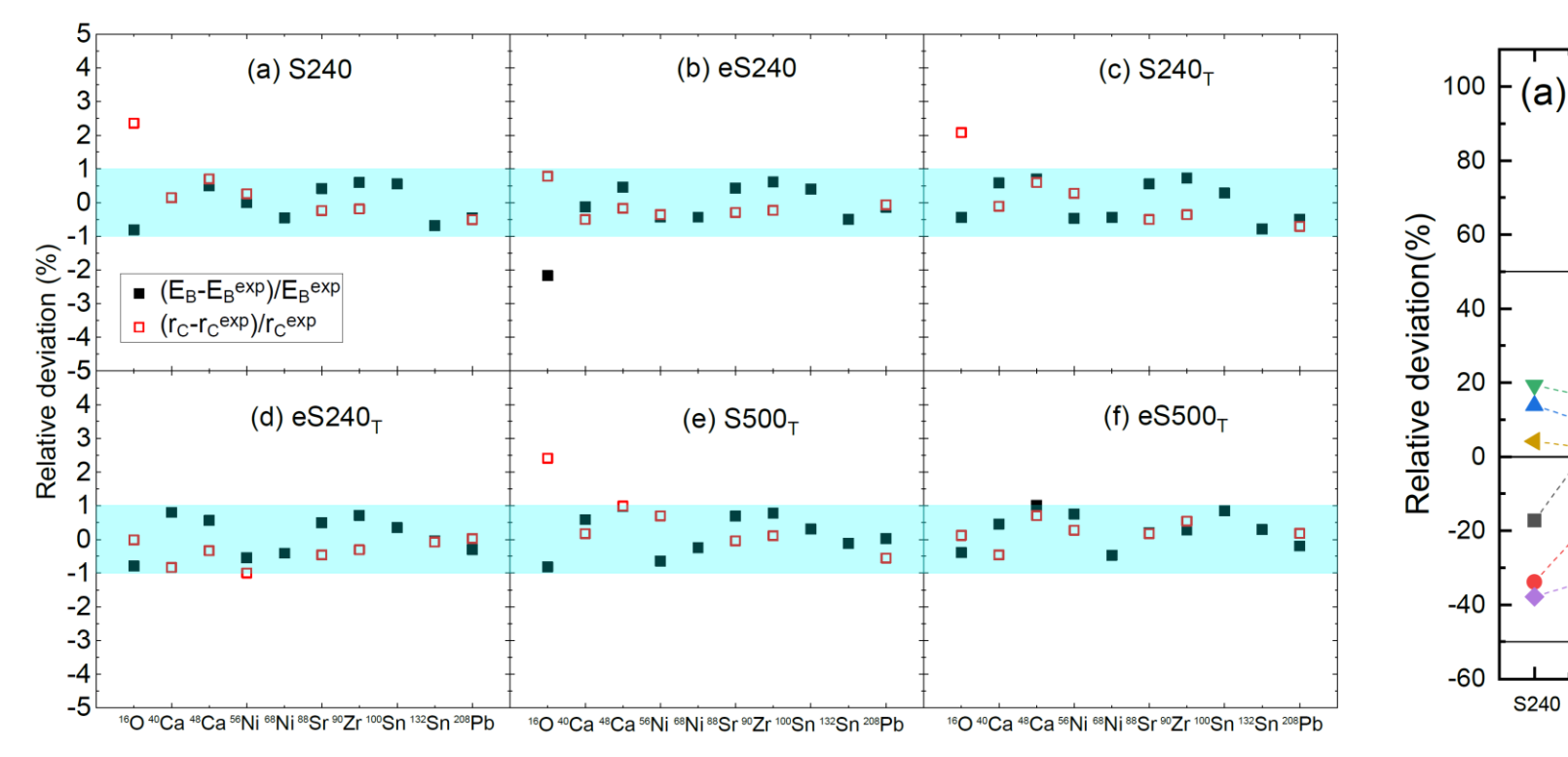
- □ The isovector spin-orbit coupling b_{IV} should be larger than ~ 240 MeV fm⁵ to fit CREX/PREX data (b_{IV} ~60 MeV fm⁵ in conventional non-relativistic EDFs. Note: b_{IS} ~120 MeV fm⁵)
- Neutrons and protons have very different spin-orbit interaction strength! (b_{IV}~ 240 MeV fm⁵ versus b_{IS}~120 MeV fm⁵)

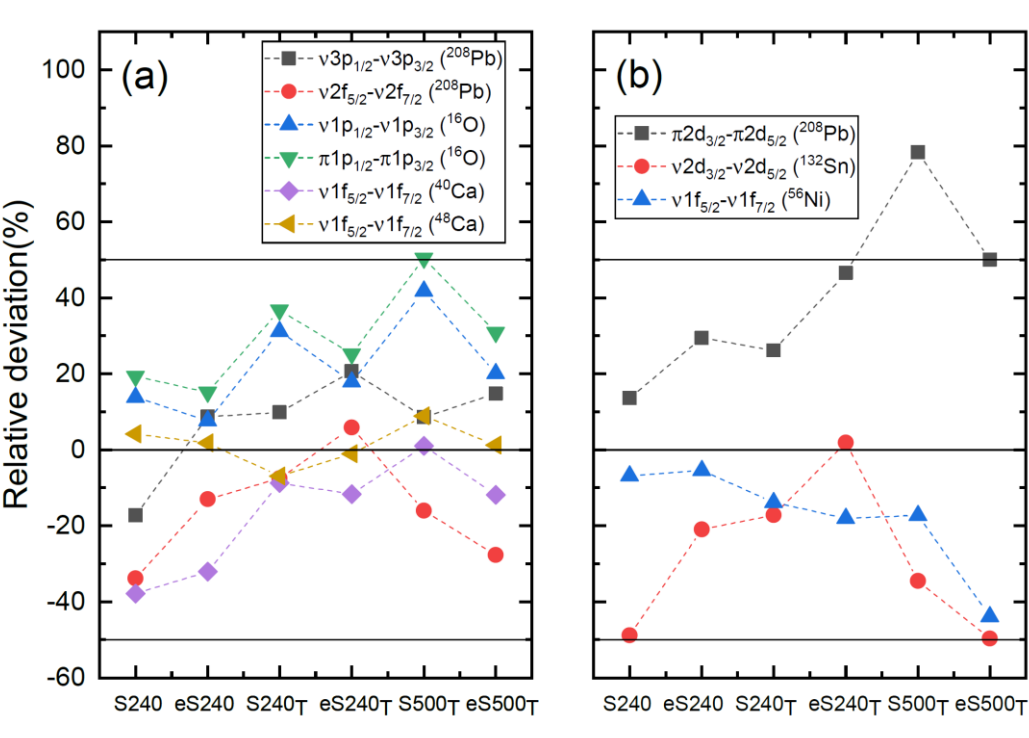
	S240	eS240	$S240_{\mathrm{T}}$	$eS240_{T}$	$S500_{\mathrm{T}}$	$eS500_{\mathrm{T}}$
$ ho_0$	0.16359	0.15580	0.16498	0.15442	0.16342	0.15089
E_0	-16.147	-16.170	-16.220	-16.190	-16.288	-15.957
$ar{m}_{s,0}$	0.982	0.939	0.993	0.865	1.022	0.921
$ar{m}_{v,0}$	0.816	0.898	0.883	0.765	0.602	0.662
S	34.08	34.45	35.19	34.06	39.03	36.96
L	46.6	60.5	52.7	57.4	99.7	80.6
$K_{ m sym}$	-207.4	-87.3	-190.4	-133.1	-101.1	-189.5
$\Delta F_{\mathrm{CW}}^{208}$	0.0280	0.0288	0.0291	0.0287	0.0400	0.0408
$\Delta F_{\mathrm{CW}}^{48}$	0.0329	0.0312	0.0321	0.0310	0.0291	0.0288
$\Delta r_{ m np}^{208}$	0.189	0.195	0.194	0.195	0.263	0.273
$\Delta r_{ m np}^{ m np}$	0.139	0.090	0.128	0.099	0.100	0.105
$lpha_{ m D}^{208}$	19.35	20.15	19.51	20.20	22.77	22.98
α_{D}^{48}	2.29	2.29	2.29	2.23	2.68	2.85

- S500T and eS500T overpredict the measured electric dipole polarizability alphaD at RCNP
 - S240/eS240/S240T/eS240T: $Nskin(Pb208) \sim 0.19 \text{ fm}, Nskin(Ca48) \sim 0.12 \text{ fm}$ $E_{sym}(\rho_0) \sim 34 \text{ MeV}, L \sim 55 \text{ MeV}$ (Nicely agree with World Average Values!)



Tong-Gang Yue/Zhen Zhang/CLW, arXiv:2406.03844





The new EDFs with strong isovector spin-orbit interaction can well describe the nuclear global properties of typical (semi)-closed shell nuclei!



T.Q. Zhao et al., arXiv:2406.05267

Characterizing the nuclear models informed by PREX and CREX: a view from Bayesian inference

Tianqi Zhao, ^{1,2,*} Zidu Lin, ^{3,†} Bharat Kumar, ^{4,‡} Andrew W. Steiner, ^{3,5,§} and Madappa Prakash^{2,¶}

¹Department of Physics, University of California Berkeley, Berkeley, California 94720, USA

²Department of Physics and Astronomy, Ohio University, Athens, Ohio 45701, USA

³University of Tennessee, Knoxville, Tennessee 37996, USA

⁴Department of Physics & Astronomy, National Institute of Technology, Rourkela 769008, India

⁵Physics Division, Oak Ridge National Laboratory

(Dated: June 11, 2024)

New measurements of the weak charge density distributions of 48 Ca and 208 Pb challenge existing nuclear models. In the post-PREX-CREX era, it is unclear if current models can simultaneously describe weak charge distributions along with accurate measurements of binding energy and charge radii. In this letter, we explore the parameter space of relativistic and non-relativistic models to study the differences between the form factors of the electric and weak charge distributions, $\Delta F = F_{ch} - F_w$, in 48 Ca and 208 Pb. We show, for the first time, the parts of the mean-field models which are the most important in determining the relative magnitude of the neutron skin in lead and calcium nuclei. We carefully disentangle the tension between the PREX/CREX constraints and the ability of the RMF and Skyrme models to accurately describe binding energies and charge radii. We find that the nuclear symmetry energy coefficient S_V and the isovector spin-orbit coefficient b_4^{\prime} play different roles in determining ΔF of 48 Ca and 208 Pb. Consequently, adjusting S_V or b_4^{\prime} shifts predicted ΔF values toward or away from PREX/CREX measurements. Additionally, S_V and the slope L are marginally correlated given the constraints of our Bayesian inference, allowing us to infer them separately from PREX and CREX data.

PHYSICAL REVIEW C 112, 014310 (2025)

Editors' Suggestion

Role of the isovector spin-orbit potential in mitigating the CREX-PREX dilemma

Athul Kunjipurayil and J. Piekarewicz Department of Physics, Florida State University, Tallahassee, Florida 32306, USA

Marc Salinas @

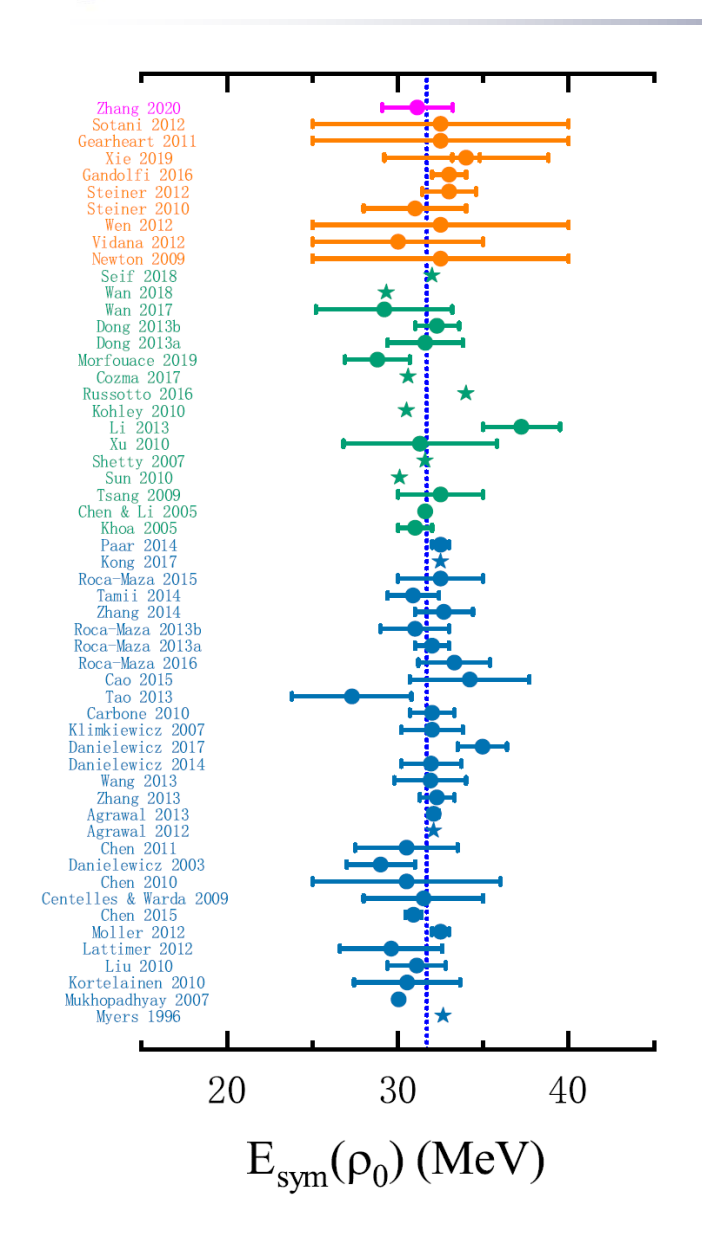
Lawrence Livermore National Laboratory, Livermore, California 94550, USA

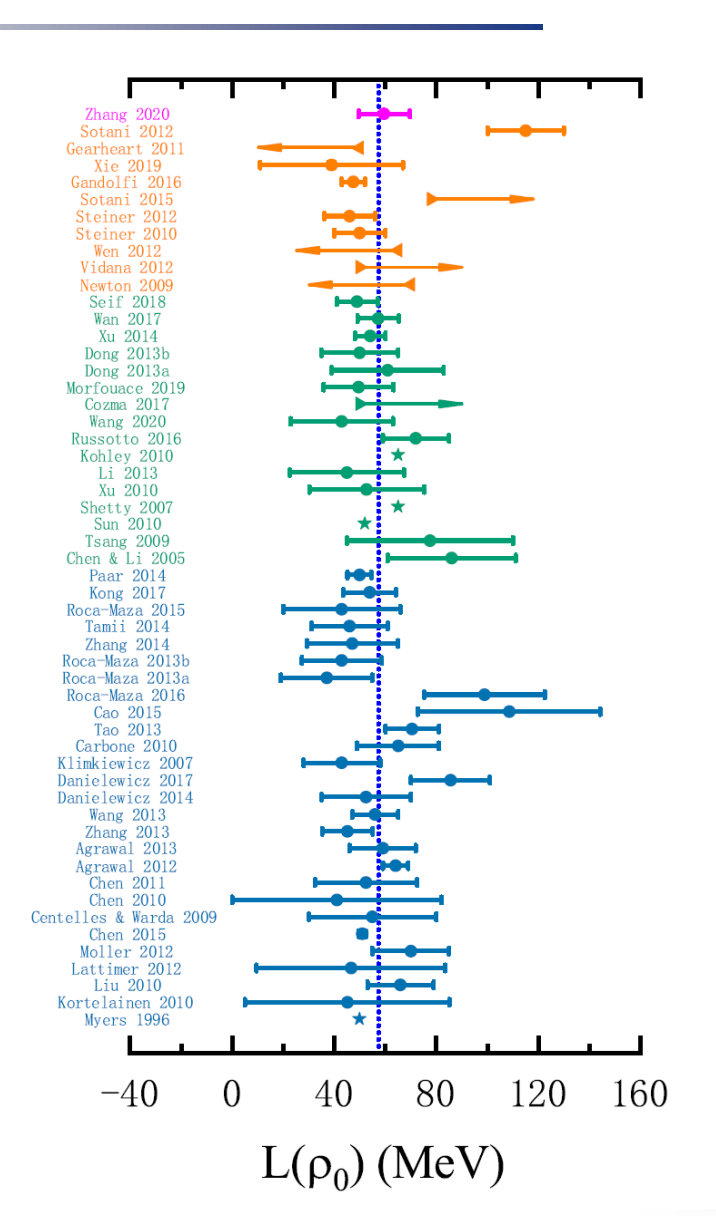
Pioneering electroweak measurements of the neutron skin thickness in lead-208 and calcium-48 are challenging our understanding of nuclear dynamics. Many theoretical models suggest that the slope of the symmetry energy controls the development of a neutron skin in neutron-rich nuclei. This led to the expectation that if lead-208 exhibits a large neutron skin, calcium-48 should as well. Given that the PREX Collaboration reported a relatively thick neutron skin in lead, we anticipated that calcium would also have a significant neutron skin. Instead, the CREX Collaboration reported a thin neutron skin in calcium. Although many suggestions have been proposed, the "CREX-PREX dilemma" remains unsolved. Recently, an intriguing scenario has emerged, suggesting that an enhanced isovector spin-orbit interaction could simultaneously account for both results. Following this approach, we performed relativistic mean-field calculations with an increased isovector spin-orbit potential. Our findings indicate that, while this modification significantly affects the structure of calcium-48, it has only a marginal impact on lead-208, thereby bringing the results into better agreement with experiment. However, the strong enhancement required to mitigate the CREX-PREX dilemma destroys the agreement with a successful spin-orbit phenomenology, primarily by modifying the well-known ordering of spin-orbit partners.

The effects of isovector spin-orbit interaction have been confirmed by other works.
b _{IV} ~ 240 MeV fm ⁵ does NOT destroy spin-orbit phenomenology in our self-consistent Skyrme
EDF calculations, although $b_{IV} \sim 500$ MeV fm ⁵ DOES (also violates the measured α_D at RCNP)!
A self-consistent covariant Point-Coupling EDF also confirms our conclusions
(Qiu/Yue/Zhang/Chen, in preparation)



E_{sym}: Around saturation density





LWC et al., Invited Review
58 analyses of terrestrial nuclear
experiments and astrophysical
observations

$$E_{\text{sym}}(\rho_0) = 31.7 \pm 3.1$$

 $L = 57.5 \pm 24.5 \text{ MeV}$

Similar conclusion has been obtained in:

- ◆ B. A. Li and X. Han, Phys. Lett. B727, 276 (2013);
- ◆ M. Oertel, M. Hempel, T. Klahn, and S. Typel, Rev. Mod. Phys. 89, 015007 (2017).



Assuming all the constraints are equally reliable !!!

With strong IVSO interaction: PREX-II/CREX data suggest $L \sim 55$ MeV



上海交通大學 SHANGHAI JIAO TONG UNIVERSITY CREX/PREX: Strong Isovector Spin-Orbit Interaction

Some implications

- □ Relativistic view: Isovector mesons (Fock) exchange, tensor coupling, ...
- □ Such a strong isovector spin-orbit interaction is expected to have significant impacts on essentially all properties of neutron-rich nuclei: The location of neutron-drip line, shell evolution in exotic nuclei, the new magic number, the properties of superheavy nuclei, ...
- **□** Future PVES for some stable nuclei (MREX/MESA):

Pb208, Ni62,...: Not sensitive to the isovector Spin-Orbit interactions (Esym);

Ca48, Zr90,...: Sensitive to the isovector Spin-Orbit interactions (isovector

spin-orbit coupling **b**_{IV})



Outline

- □ The Symmetry Energy (Esym)
 □ Neutron Skin (Nskin): CREX/PREX puzzle
 □ Isovector Spin-Orbit Interaction
- Summary and outlook

Summary and Outlook

 PREX-II/CREX puzzle can be solved by introducing a strong isovector Spin-Orbit interaction (four times larger than conventional EDFs)!

```
Nskin(Pb208) ~ 0.19 fm, Nskin(Ca48) ~ 0.12 fm E_{\rm sym}(\rho_0) ~ 34 MeV and L~55 MeV
```

- PVES experiment for more nuclei is very helpful:
 Pb208, Ni62,... are insensitive to isovector Spin-Orbit interaction
 but Ca48, Zr90,... do! --- Can simultaneously determine IVSO and Esym with minimum model dependence
- Isovector spin-orbit effects: Shell evolution, new magic numbers, ...





谢谢! Thanks!

